Electronic Supplementary Material (ESI) for Physical Chemistry Chemical Physics.

Supporting Figures

Table S1 Experimental and numerical comparison of H-bonds between ACE2-RBD. The first and second columns indicate the residues (and atoms) of respectively RBD and ACE2, involved in the formation of a H-bond, while the third column indicates the donor/acceptor length. The first three columns were computed on the minimized crystal structure [1]. Bold donor/acceptor pairs were also identified in the experimental paper [1]. The last two columns show the occurrence and the donor/acceptor length computed on the convergence interval (250-500 ns) of our MD of the ACE2/RBD complex.

Hydrogen Bonds				
RBD's atom	ACE2's atom	EXP length (Å)	MD occurrence (%)	MD length (Å)
K417(NZ)	D30(OD1)	2.7	17.16	2.89 ± 0.19
K417(NZ)	**D30(OD2)**	2.7	25.74	2.84 ± 0.16
Y449(OH)	D38(OD2)	2.6	40.64	2.73 ± 0.18
E484(OE2)	K31(NZ)	2.8	0.01	2.86 ± 0.07
N487(ND2)	**Q24(OE1)**	2.8	3.06	2.92 ± 0.16
N487(OD1)	**Y83(OH)**	2.7	5.06	2.85 ± 0.18
Y489(OH)	**Y83(OH)**	2.8	12.95	3.33 ± 0.99
Q493(OE1)	K31(NZ)	2.9	34.82	2.80 ± 0.11
Q493(NE2)	E35(OE1)	2.7	36.95	2.89 ± 0.16
Q498(NE2)	D38(OD2)	2.9	9.57	2.95 ± 0.21
Q498(NE2)	Q42(NE2)	3.0	0.61	3.19 ± 0.17
Q498(NE2)	Q42(OE1)	3.1	0.30	2.98 ± 0.14
T500(O)	N330(ND2)	3.0	0.00	-
T500(OG1)	D355(OD2)	2.7	7.34	2.84 ± 0.22
Y505(OH)	**E37(OE2)**	2.6	27.59	2.76 ± 0.19

Notes and references

1 J. Lan, J. Ge, J. Yu, S. Shan, H. Zhou, S. Fan, Q. Zhang, X. Shi, Q. Wang, L. Zhang *et al.*, *Nature*, 2020, **581**, 215–220.

2 Schrödinger, LLC, PyMOL: The PyMOL Molecular Graphics System, Version 1.8, Schrödinger, LLC.

3 O. Trott and A. J. Olson, *Journal of computational chemistry*, 2010, **31**, 455–461.

4 A. C. Wallace, R. A. Laskowski and J. M. Thornton, *Protein engineering, design and selection*, 1995, **8**, 127–134.

5 R. A. Laskowski and M. B. Swindells, *LigPlot+: multiple ligand–protein interaction diagrams for drug discovery*, 2011.

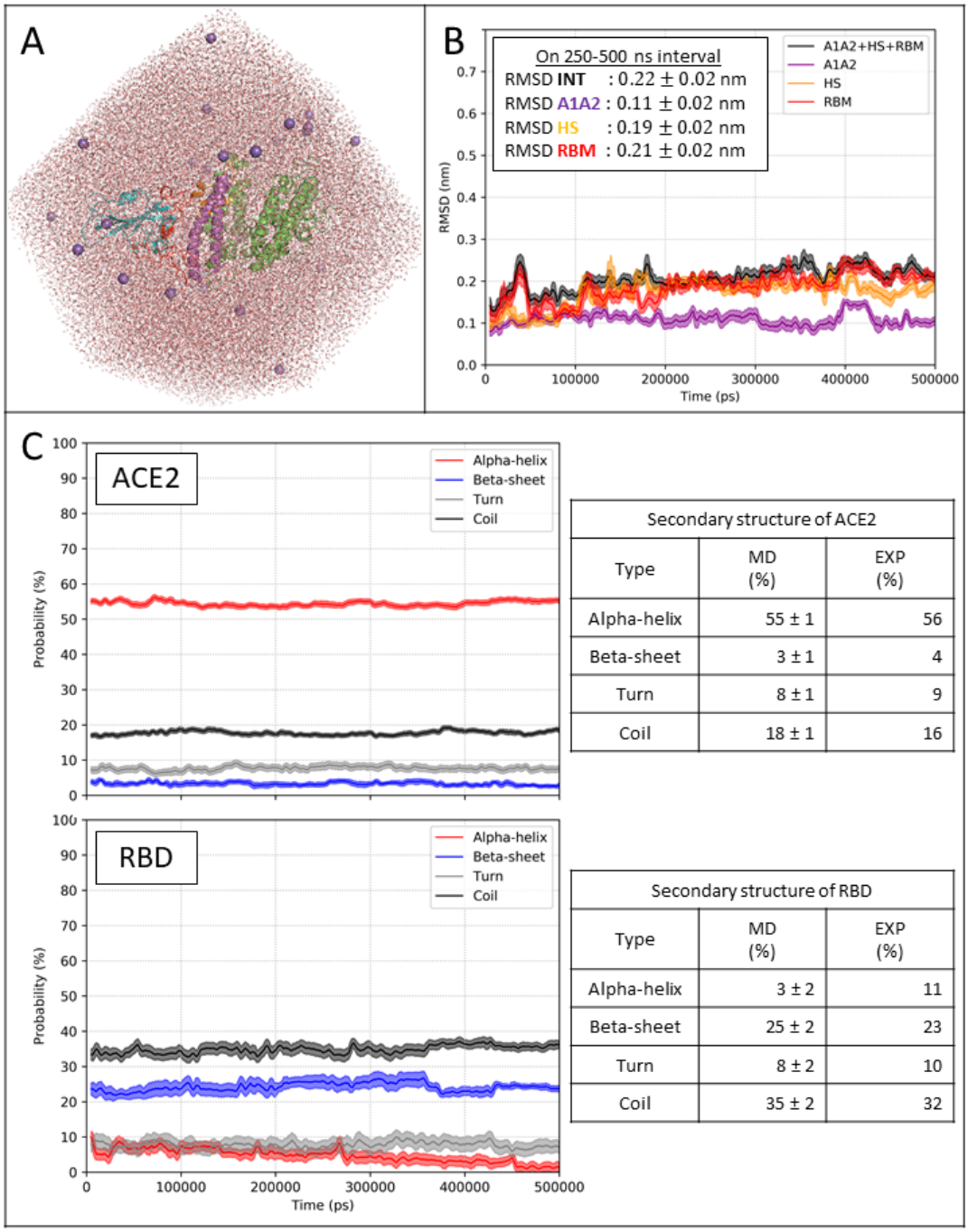

Secondary structure of ACE2		
Type	MD (%)	EXP (%)
Alpha-helix	55 ± 1	56
Beta-sheet	3 ± 1	4
Turn	8 ± 1	9
Coil	18 ± 1	16

Secondary structure of RBD		
Type	MD (%)	EXP (%)
Alpha-helix	3 ± 2	11
Beta-sheet	25 ± 2	23
Turn	8 ± 2	10
Coil	35 ± 2	32

Fig. S1 Convergence of the ACE2-RBD complex MD simulation. (A) The simulated system with ACE2 in magenta (A1A2, residues 19-83), orange (HS, residues 322-362) and green (else) as well as RBD in red (RBM, residues 438-506) and teal (else). **(B)** Root mean square deviation (RMSD) on the backbone atoms (N, Cα, C and O) from the experimental crystal structure of the complex (PDB:6M0J) as a function of time for the regions at the interface (A1A2 and HS for ACE2 and RBM for RBD). The average and the standard deviation of the RMSD on the converged interval (250-500 ns) are shown in the inset. **(C)** The DSSP secondary structure as a function of time for ACE2 and RBD. The average and the standard deviation of the secondary structure on the converged interval are compared to the values computed on the experimental structure (EXP) on the right side. Only the α-helix, β-sheet, turn and coil content are shown. The difference with 100% is associated rest of the DSSP secondary structure classes (β-bridge, bend, 310-helix and π-helix). **(B-C)** The figures depict the running average using a 5-ns time window. The $\pm 1\sigma$ interval is shown by the semitransparent region around the curve.

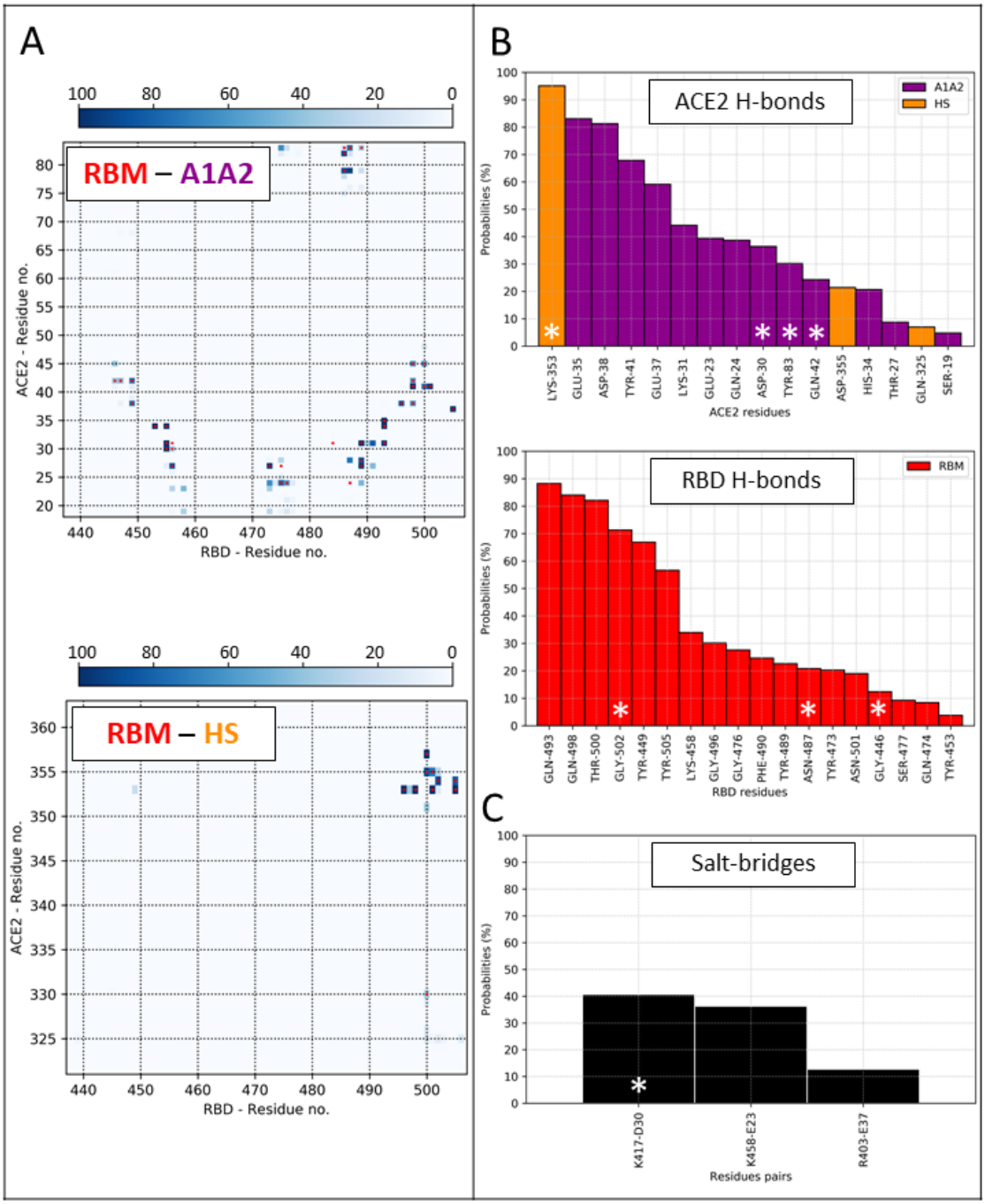

Fig. S2 Contacts between ACE2 and RBD during the MD simulation. (A) Probability contact maps between A1A2 (residues 19-83 of ACE2) and RBM (residues 438-506 of RBD) as well as between HS (residues 322-362 of ACE2) and RBM (residues 438-506 of RBD). A contact is considered between two residues if the distance between any pair of atoms is smaller than 0.40 nm. The presence of a contact in the experimental crystal complex (PDB:6M0J) is shown by a red dot. **(B)** H-bonds probability of ACE2 residues with RBD (top) and of RBD residues with ACE2 (bottom). A H-bond is considered when the donor-acceptor distance is less than 0.35 nm and when the hydrogen-donor-acceptor angle is less than 35 degrees. The involvement of each residue in a H-bond in the experimental crystal structure is indicated by the white star. **(C)** Salt-bridges probability of ACE2 with RBD. A salt-bridge is considered when the distance between two oppositely charged groups is less than 0.40 nm. The presence of the salt-bridges in the crystal structure is shown by the white star. **(A-B-C)** All probabilities are computed on the converged interval (250-500 ns).

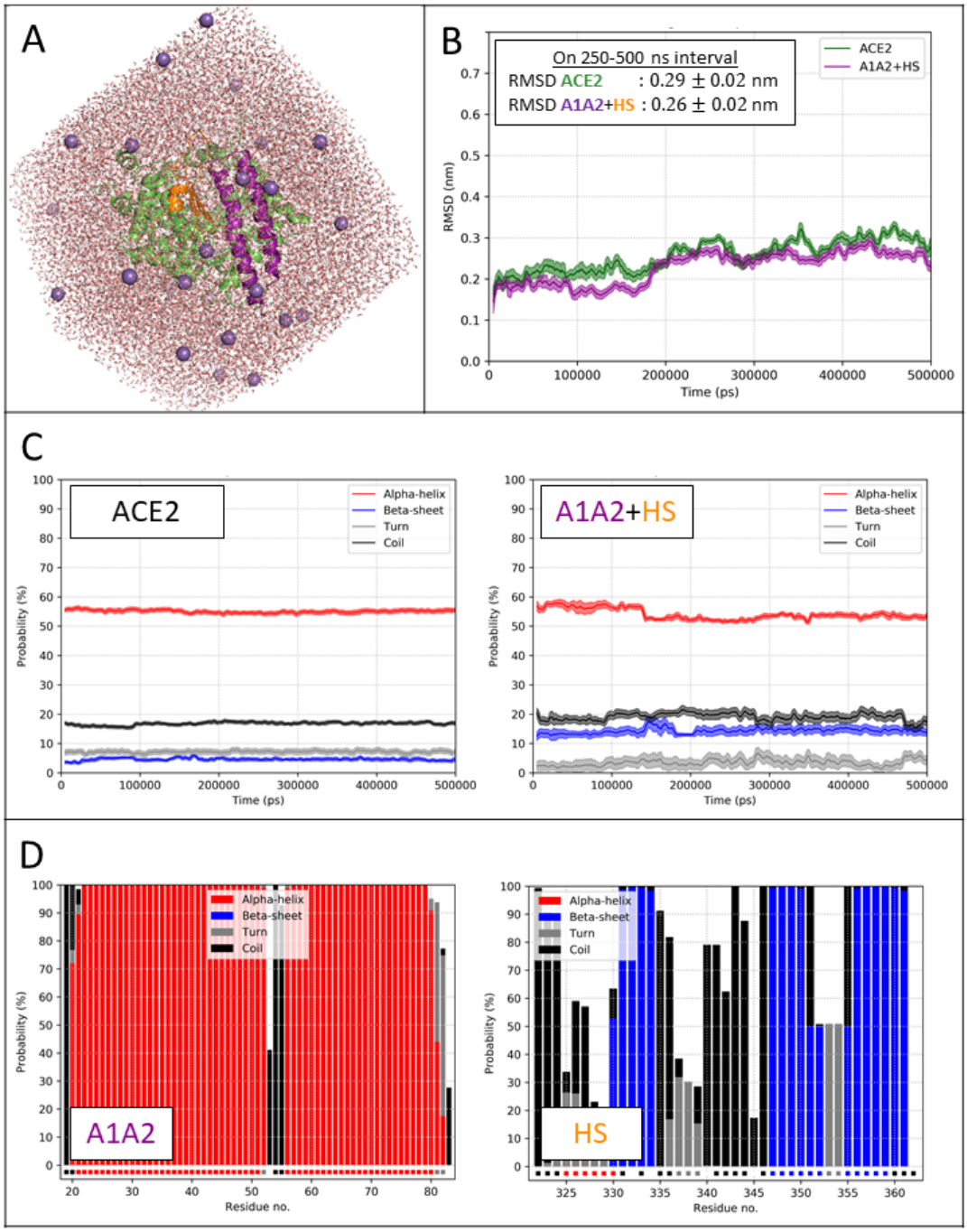

Fig. S3 Convergence of the ACE2 MD simulation. (A) The simulated system with ACE2 in magenta (A1A2, residues 19-83), orange (HS, residues 322-362) and green (else). **(B)** Root mean square deviation (RMSD) on the backbone atoms (N, Cα, C and O) from the structure of ACE2 in the experimental crystal of the complex (PDB:6M0J) as a function of time for the whole protein (ACE2) and the regions at the interface (A1A2 and HS). The average and the standard deviation of the RMSD on the converged interval (250-500 ns) are shown in the inset. **(C)** The DSSP secondary structure as a function of time for ACE2 (left) and A1A2+HS (right). **(B-C)** The figures depict the running average using a 5-ns time window. The $\pm 1\sigma$ interval is shown by the semitransparent region around the curve. **(D)** The DSSP per residue secondary structure for A1A2 (left) and HS (right) on the converged interval (250-500 ns). The experimental secondary structure for each residue is illustrated by the square below the 0 mark. White means other secondary structure.

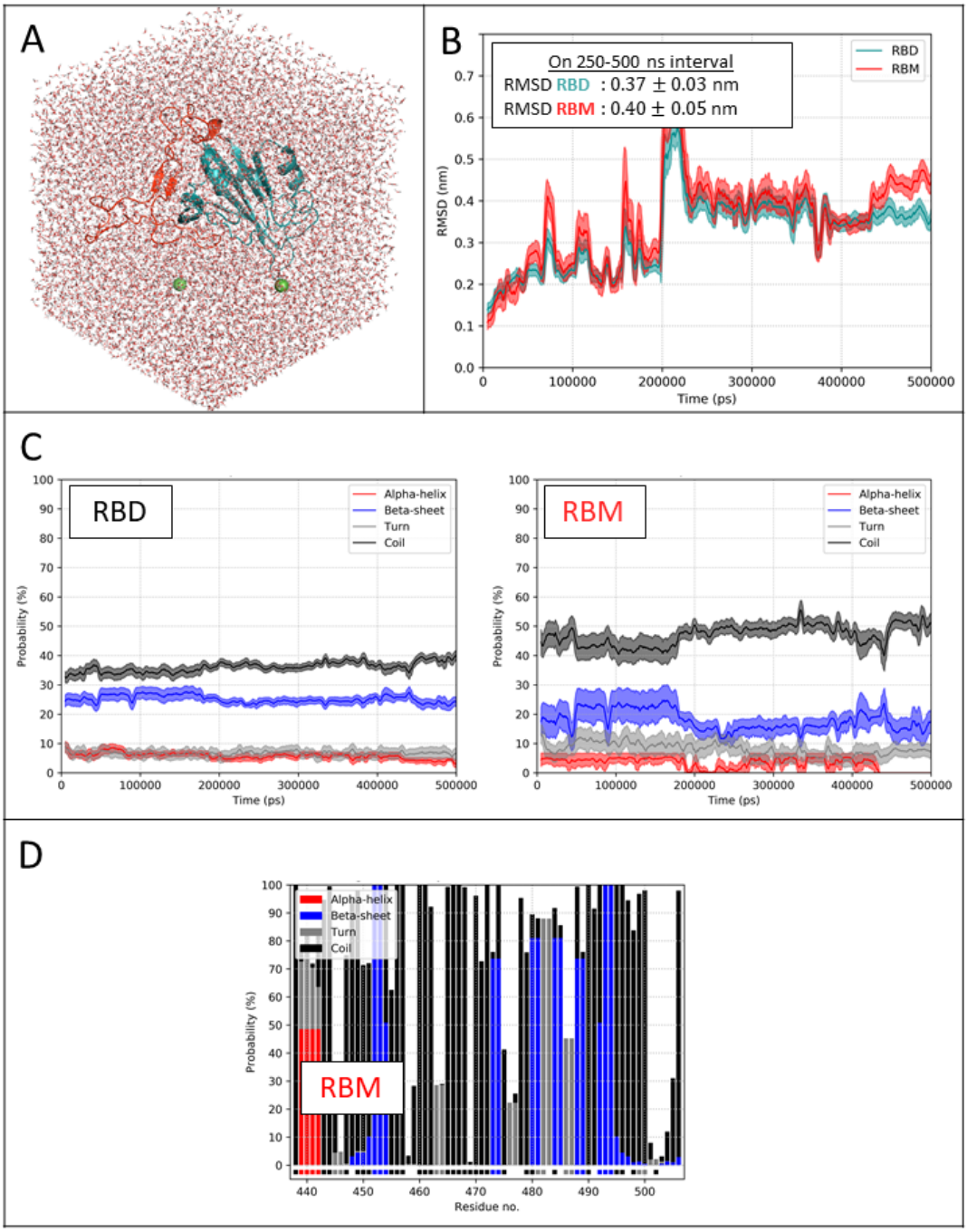

Fig. S4 Convergence of the RBD MD simulation. (A) The simulated system with RBD in red (RBM, residues 438-506) and teal (else). **(B)** Root mean square deviation (RMSD) on the backbone atoms (N, Cα, C and O) from the structure of RBD in the experimental crystal of the complex (PDB:6M0J) as a function of time for the whole protein (RBD) and the region at the interface (RBM). The average and the standard deviation of the RMSD on the converged interval (250-500 ns) are shown in the inset. **(C)** The DSSP secondary structure as a function of time for RBD (left) and RBM (right). **(B-C)** The figures depict the running average using a 5-ns time window. The $\pm 1\sigma$ interval is shown by the semitransparent region around the curve. **(D)** The DSSP per residue secondary structure for RBM on the converged interval (250-500 ns). The experimental secondary structure for each residue is illustrated by the square below the 0 mark. White means other secondary structure.

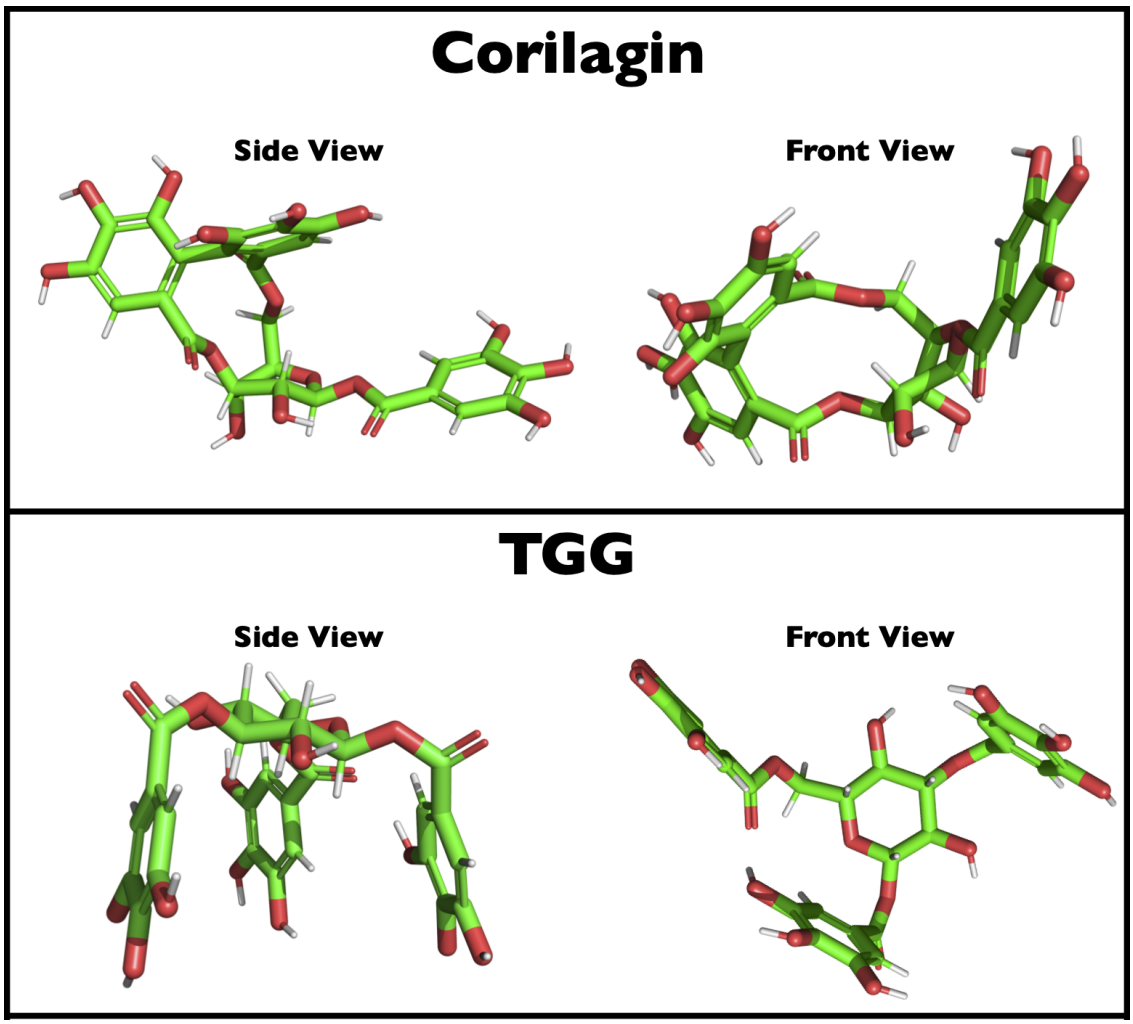

Fig. S5 The initial structure of each ligand. (TOP) Corilagin (BOTTOM) TGG. The figures were generated using PyMOL[2].

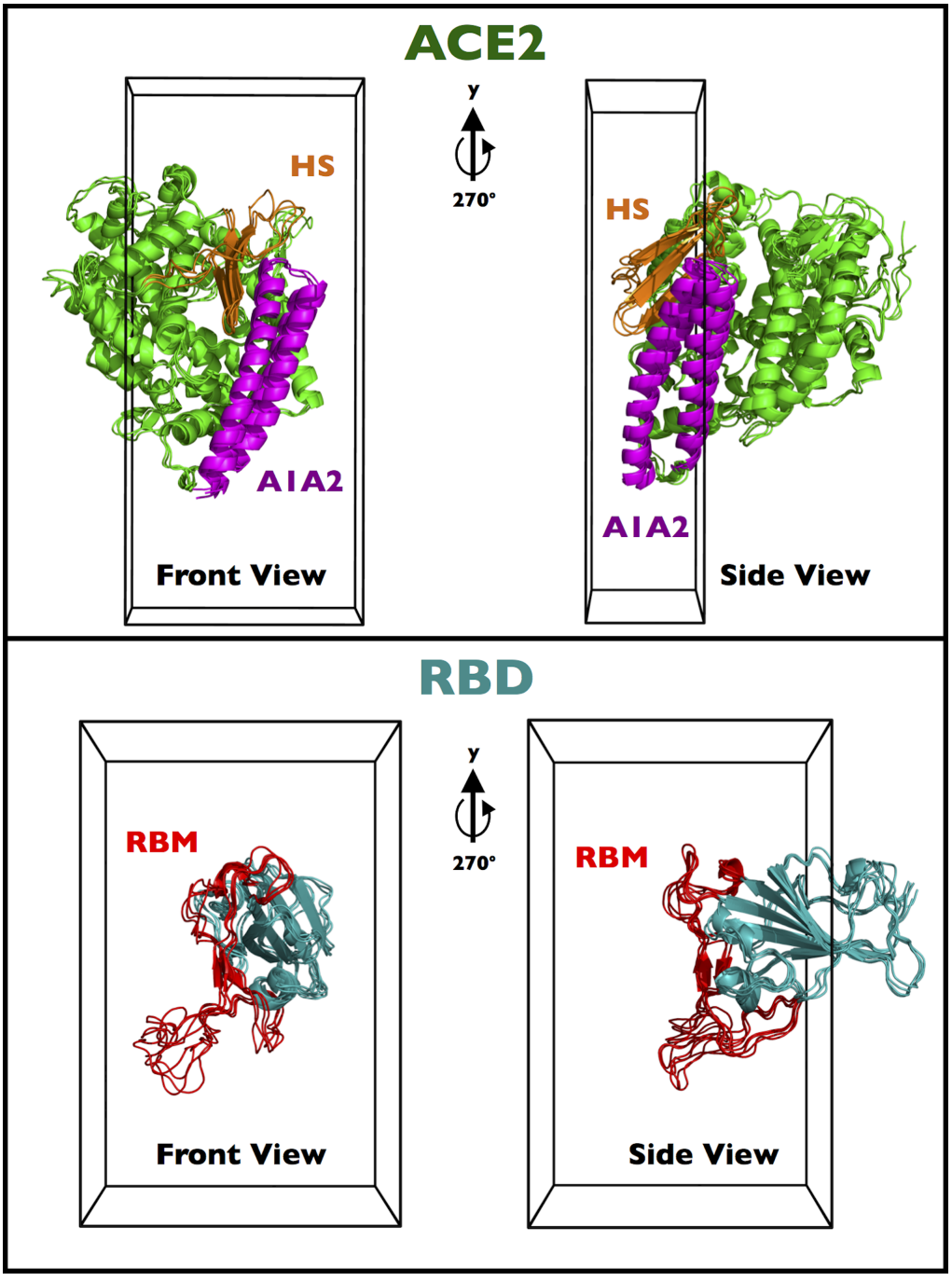

Fig. S6 Configuration ensembles and box used for the molecular docking. (Top) Box used for the docking on ACE2. The box is centered around the point (6.5427, 8.3338, 6.5367) nm with a size of 2.2640 nm, 5.2072 nm, 1.4633 nm respectively in x, y and z. The A1A2 region (residues 19-83) and the HS region (residues 322-362) are shown respectively in magenta and orange. **(Bottom)** Box used for docking on the RBD. The box is centered around the point (6.13835, 6.8906, 1.1736) nm with a size of 2.7625 nm, 4.3358 nm, 2.6026 nm respectively in x, y and z. The RBM segment (residues 438-506) is shown in red.

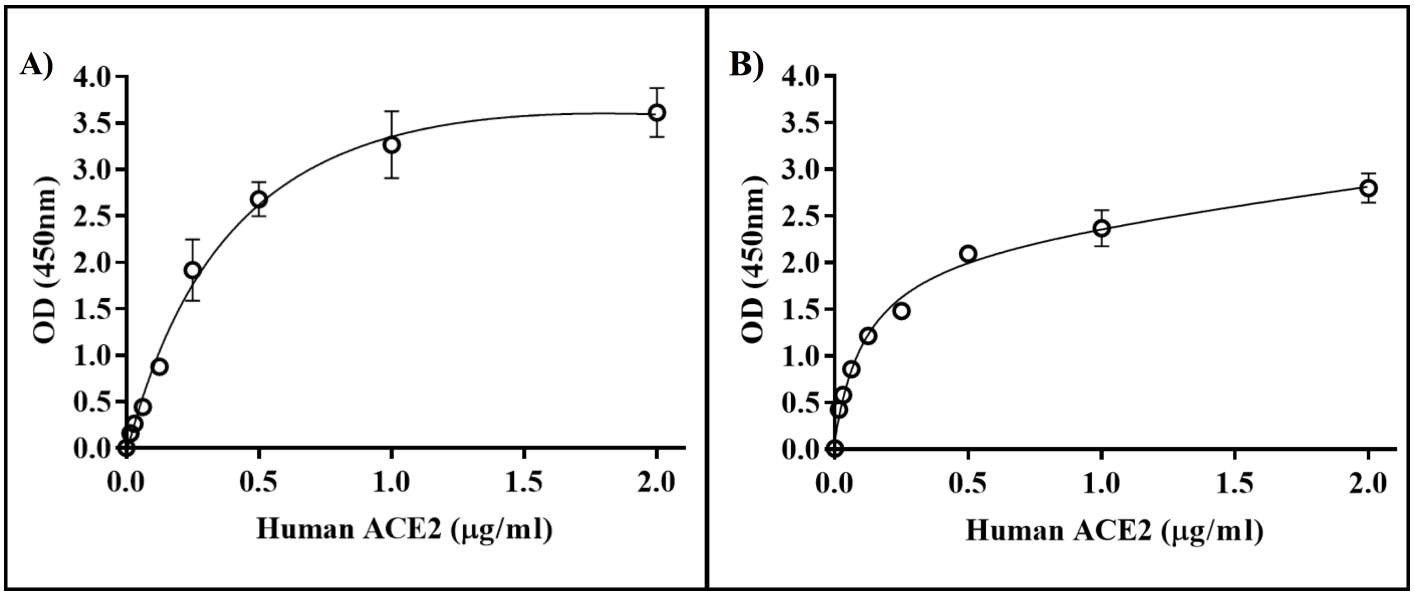

Fig. S7 A) Human ACE2 protein binding to immobilized SARS-CoV-2 RBD Spike protein (0.5 μg/ml) using an increasing dose of human ACE2 protein (0,015 to 2 μg/ml). **B) Human ACE2 protein binding to immobilized ACE2 antibody** (0.5 μg/ml) using an increasing dose of human ACE2 protein (0,015 to 2 μg/ml). Results are expressed as mean $\pm$ standard error.

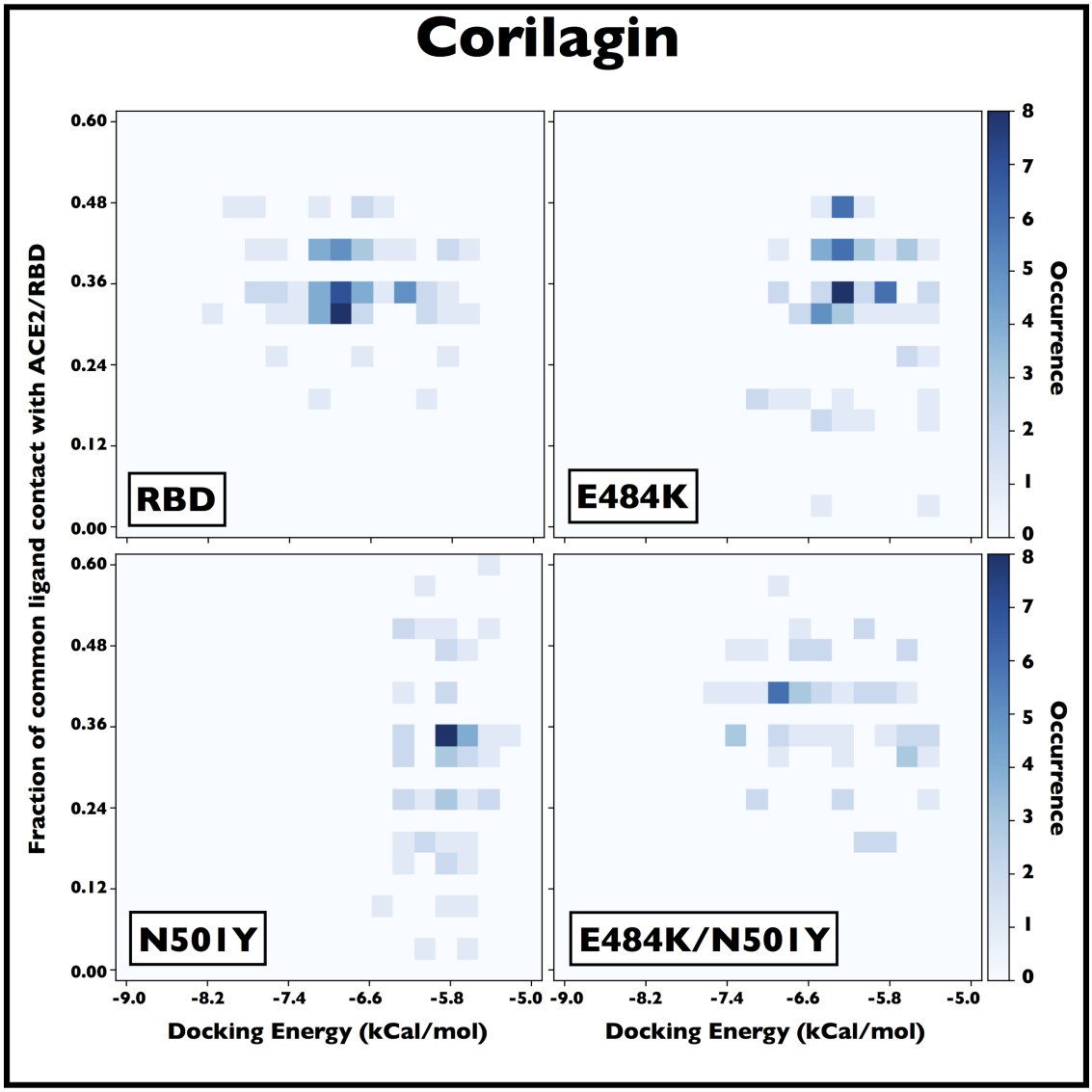

Fig. S8 Corilagin's ability of the generated docking conformations to block the ACE2-RBD complex formation. The docking conformations generated by AutoDock VINA[3] as a function of its binding energy (x-axis) and fraction of ACE2/RBD contacts such conformation is able to black (y-axis). The occurrence of such conformation is shown as the z-axis.

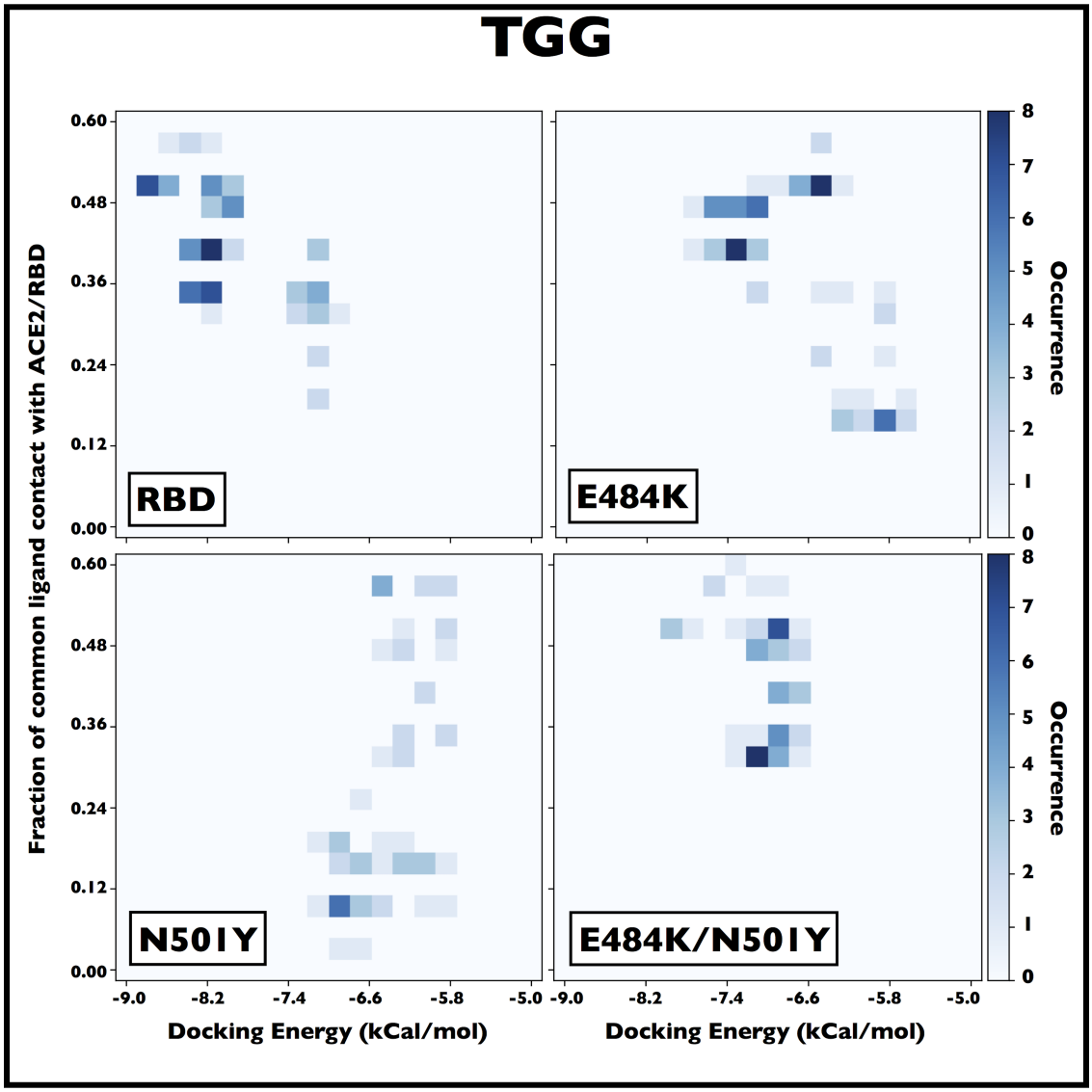

Fig. S9 TGG's ability of the generated docking conformations to block the ACE2-RBD complex formation. The docking conformations generated by AutoDock VINA[3] as a function of its binding energy (x-axis) and fraction of ACE2/RBD contacts such conformation is able to black (y-axis). The occurrence of such conformation is shown as the z-axis.

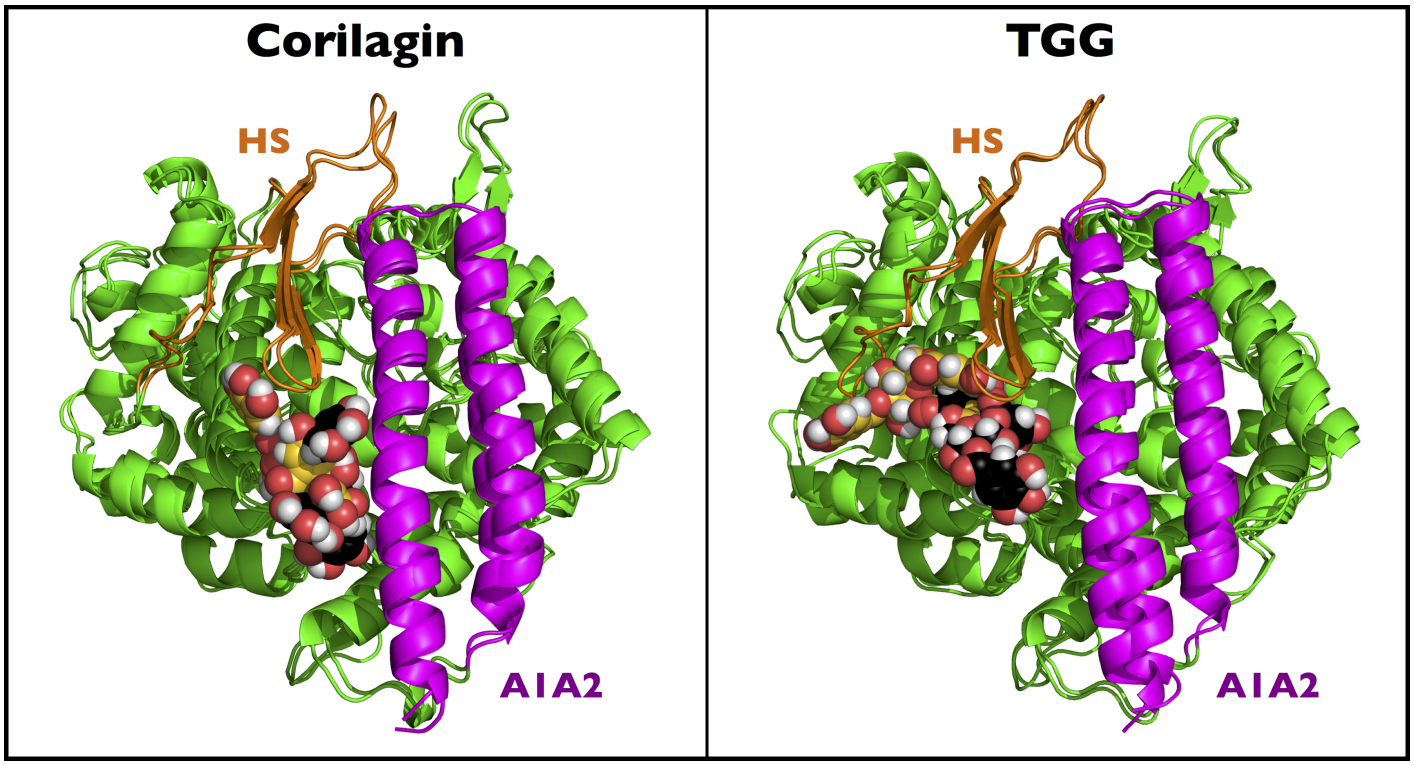

Fig. S10 Ligands poses on ACE2. The docked position of corilagin (right) and TGG (left) on the ACE2 protein. The A1A2 segment, the HS segment and the rest of the RBD is shown in purple, orange and green respectively. The ligand in black and gold is respectively the conformation after docking and the center of the biggest cluster sampled during MD simulation respectively.

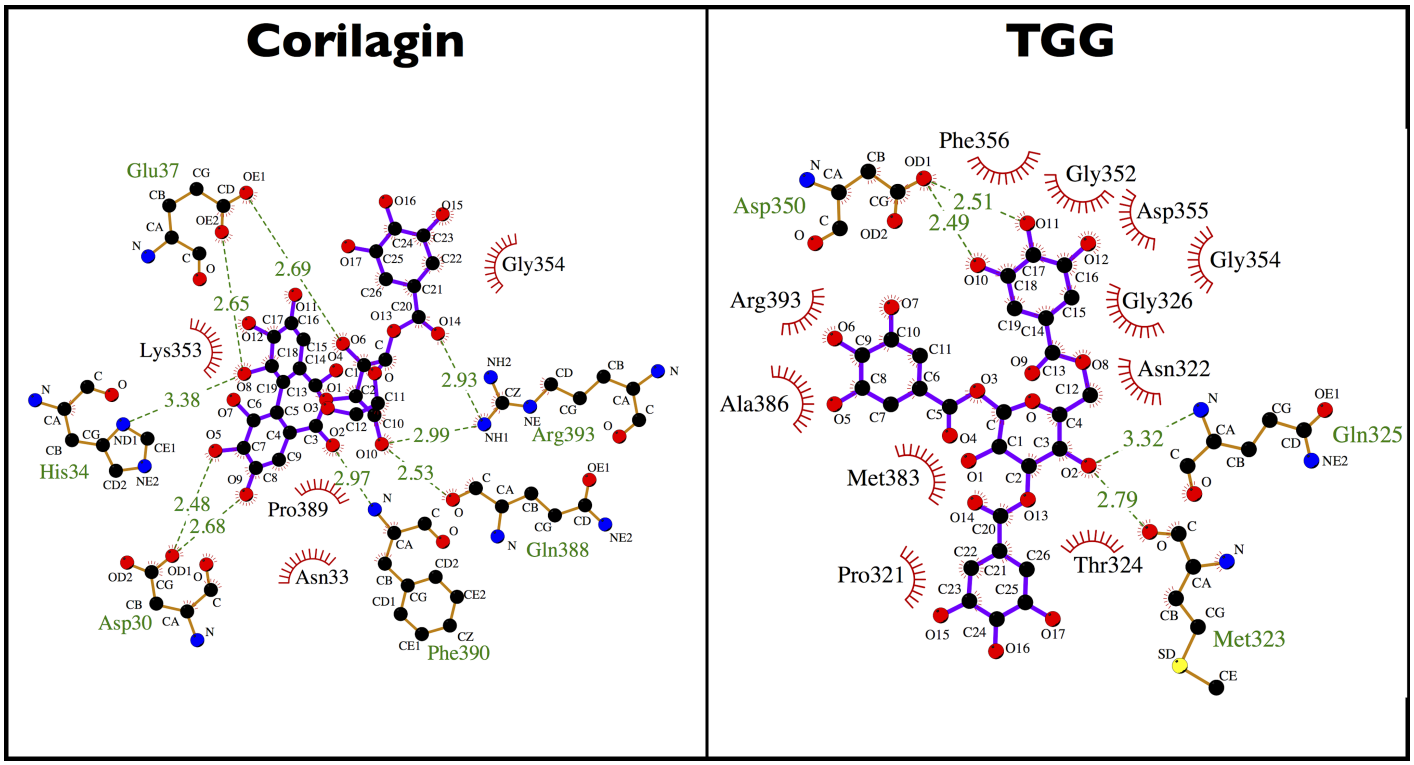

Fig. S11 Ligands interaction map with ACE2. The interaction maps of corilagin (right) and TGG (left) with ACE2 are shown for the center of the biggest cluster computed on the convergence interval using the protein backbone atoms and ligand non-hydrogen atoms. The nonpolar contacts, defined by a distance smaller than 0.40 nm, between the ligand and the protein are shown as red arcs. H-bonds and their donor/acceptor distance are shown in green. All figures were generated using LIGPLOT[4,5].

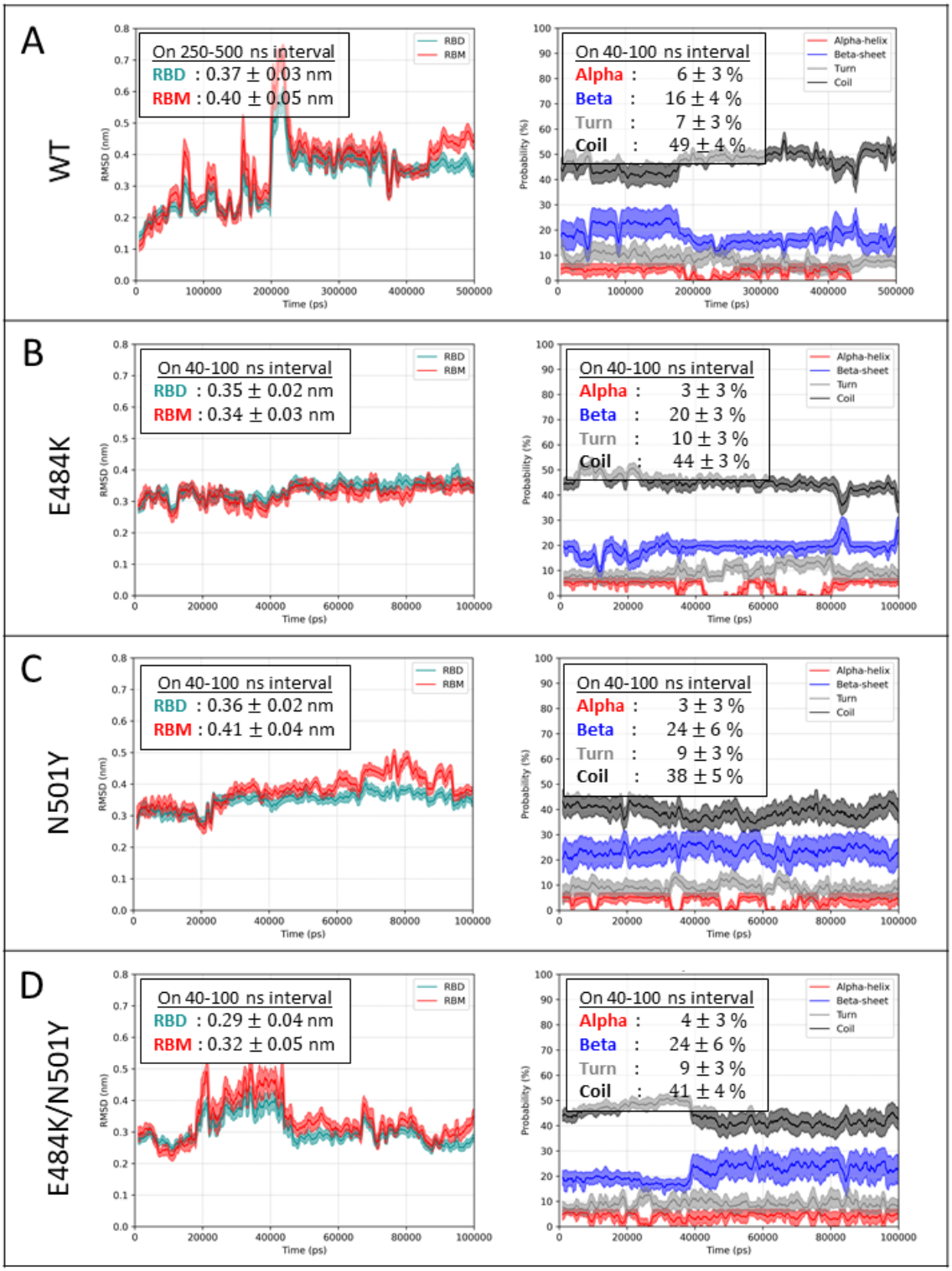

Fig. S12 Convergence of the RBD mutants MD simulations. Backbone RMSD on the N, Cα, C and O atoms from the wild-type experimental structure and DSSP secondary structure as a function of time for (A) wildtype RBD, (B) E484K, (C) N501Y and (D) E484K/N501Y mutations.

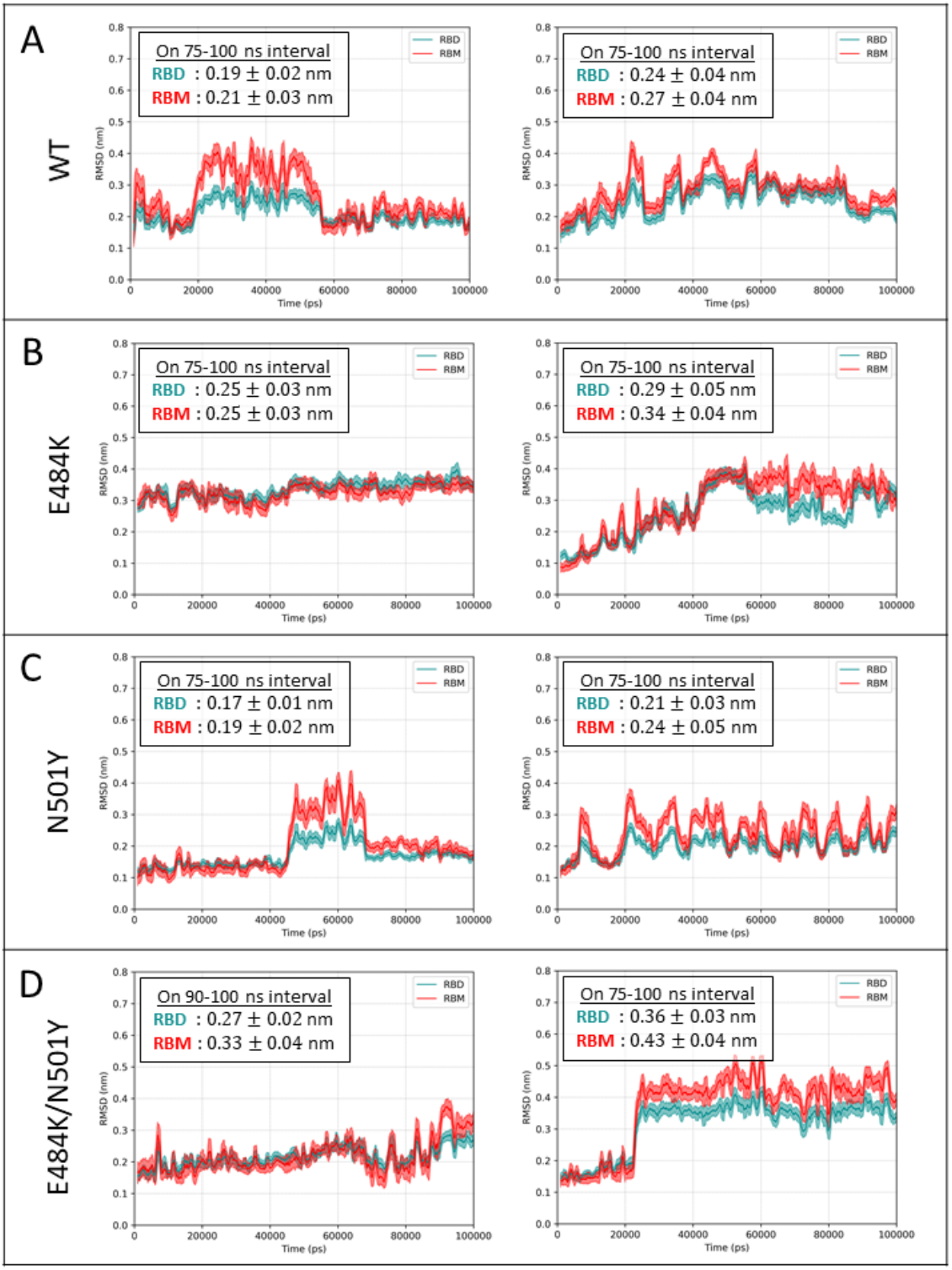

Fig. S13 Convergence of the ligands–RBD MD simulations. Convergence is assessed by monitoring the RMSD on the backbone atoms of RBD (N, Cα, C and O) and the non-hydrogen atoms of the ligands from the initial structure as a function of time for (A) wildtype RBD, (B) E484K, (C) N501Y and (D) E484K/N501Y mutations. To the left, corilagin–RBD. To the right, TGG–RBD.

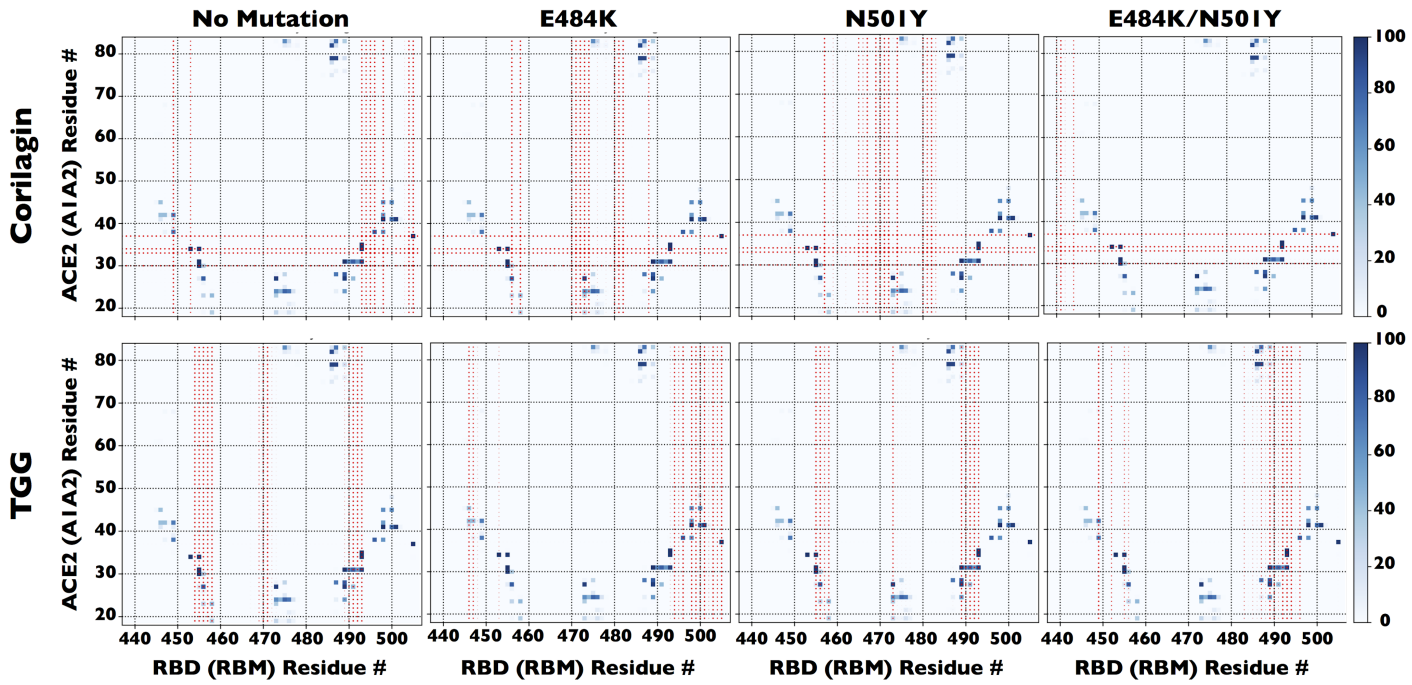

Fig. S14 Ligand-protein contact network on A1A2 and RBM. The contact probability map between the A1A2 segment of ACE2 (vertical axis) and the RBM segment of RBD (horizontal axis) is shown in blue. These probabilities were computed on the converged interval of the MD simulation on the ACE2-RBD complex. The red disks indicate the residues blocked by corilagin (top row) and TGG (bottom row) during our ligand-protein MD simulations on ACE2, RBD, RBD/E484K, RBD/N501Y and RBD/E484K-N501Y. The size of the circles is proportional to the interaction probability with the residues.

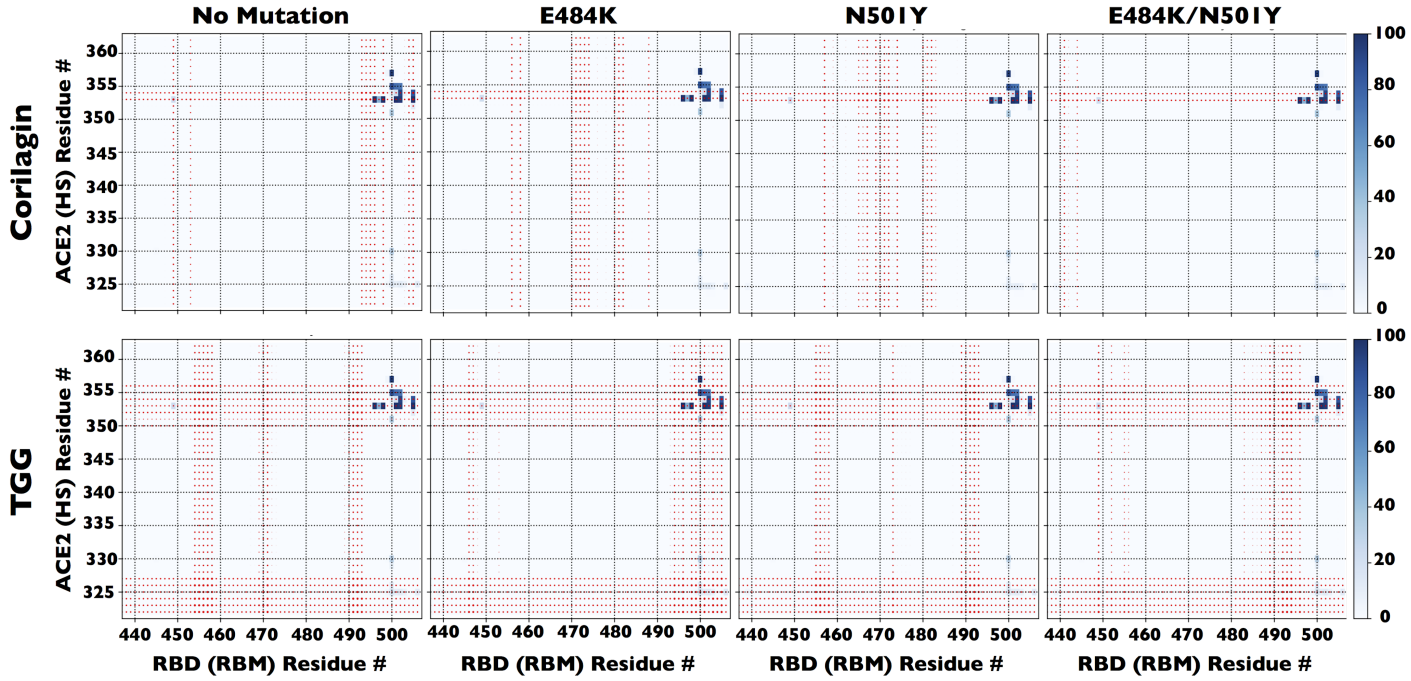

Fig. S15 Ligand-protein contact network on HS and RBM. The contact probability map between the HS segment of ACE2 (vertical axis) and the RBM segment of RBD (horizontal axis) is shown in blue. These probabilities were computed on the converged interval of the MD simulation on the ACE2-RBD complex. The red disks indicate the residues blocked by corilagin (top row) and TGG (bottom row) during our ligand-protein MD simulations on ACE2, RBD, RBD/E484K, RBD/N501Y and RBD/E484K-N501Y.